ingegneria sismica
International Journal of Earthquake Engineering
Anno XLIII - Num. 1 - 2026

Research on the technology of improving the accuracy of resource exploration in mining areas based on digital geological modeling

Tianqi Dong[1,2,*]

[1] School of Earth Sciences and Engineering, Xi'an Shiyou University, Xi'an, 710065, Shaanxi, China
[2] Shaanxi Key Laboratory of Petroleum Accumulation Geology, Xi'an Shiyou University, Xi'an, 710065, Shaanxi, China

SUMMARY: *The visual modeling technology of 3D digital geological model, as a component of CAD technology, is also a hot content of current geoscientific development research. This paper is based on the GOCAD platform, and at the same time constructs the corresponding spatial database, and establishes a three-dimensional geological model of the mining area on this basis, and uses the kriging algorithm to derive the grade trend prediction model in the area. The X mining area is taken as the study area to carry out the 3D mineralization prediction research, through the quantitative extraction of the stratigraphy, rock bodies and other mineralization factors in the area, the introduction of the weight of evidence method to construct the mineral search model, and the use of the ROC curve to evaluate the performance of the model. Through the study, four mineral searching target areas were circled in the X mining area, and the a posteriori probability of mineralization can be divided into four levels: high, higher, lower, and low, and the AUC value of the evidence weight model is 0.94, which is a better prediction performance, and the probability of finding minerals is about 78.2%.*

KEYWORDS: *three-dimensional geological modeling; GOCAD; mineralization prediction; right-of-evidence approach*

1 Introduction

With the rapid growth of global energy demand, the development and utilization of mineral resources has become an indispensable part of the economic development of various countries. Under such a background, geological exploration is particularly critical, which provides indispensable information support for the rational development of mineral resources, environmental protection and the safe operation of underground engineering [1]. Geological exploration is of key significance for the rational development and long-term operation of mining areas. Especially in complex geological structures and resource-rich mining areas, accurate and efficient geological exploration not only helps to optimize the resource development strategy, but also has a far-reaching impact on the environmental protection and the safety of underground engineering [2, 3]. In the specific application process, geological exploration is mainly carried out in the framework of manual + equipment of "field inspection, profile measurement, soil analysis", and the exploration in mining areas with complex terrain is easily disturbed by the environment, which leads to insufficient precision and low efficiency, and the development technology for deep mining areas is limited [4-7].

*dtq1234562026@163.com
https://doi.org/10.65102/is2026022
Published: 30 April, 2026

With the wide application of geological modeling methods in the field of geological exploration and the gradual accumulation of geological models, the demand for management and further application of geological models for resource exploration in mining areas has become more and more urgent [8]. Geological models experience from two-dimensional to three-dimensional, and then to the digital intelligence stage, realizing the leap from static to dynamic. Zhang et al. integrated multi-source geoscientific data and constructed a two-dimensional mineral search prediction atlas and three-dimensional mineralization model from surface to -3000 m depth, found that the Early Cretaceous intrusive body is the key ore-controlling factor, and circled a new exploration target area in the western part of Sanguriu intrusive body at a depth of 1000-3000 m [9]. Chen et al. achieved an accurate estimation of deep gold resources by constructing a high-precision three-dimensional geological model of ore-control structures and optimizing the key parameters using support vector machines and martensitic distances, which was verified to be reliable in the Jiaojia and Daxingzhuang fields in Jiaodong [10]. Using the example of the Kadia lignite mine in Greece, Krassakis et al. demonstrated a set of workflows for complex geological environments in mines integrating geographic information systems (GIS) and three-dimensional geologic modeling for site selection of new types of mining methods, such as underground coal gasification, and effective support for decision-making by improving the quality of the information, thus saving time and exploration costs [11].

And digital geological model with the help of multi-source information fusion, artificial intelligence algorithms, digital twin, visualization and other technologies to examine the depth of the information of the mining area, so as to improve the accuracy of exploration. Lyu et al. fusion of multi-source remote sensing data, and the use of principal component analysis and machine learning to extract the mineralization and alteration information, and effectively identify the ore-controlling structures and anomalous zones, which provide a reliable method for the precise circling of the target area of the search for minerals [12]. Liu et al. proposed an improved iterative nearest point and intrinsic shape feature point cloud alignment algorithm to achieve the accurate fusion of multi-source data in the mining area, which significantly improved the accuracy and efficiency of the construction of the 3D geological model, with an average alignment error of less than 0.68 m [13]. Zhou and Liu integrated three-dimensional geological modeling, numerical dynamic simulation and machine learning methods to predict the mineralization of the Dongguashan ore field, showing that volumetric strain and contact zone inclination are the key ore-controlling factors, and confirming that the fusion of dynamics and geological evidence can significantly improve the accuracy of the prediction model and effectively define the target area of deep-searching for minerals [14]. Zong et al. proposed a deep learning-based method for intelligent identification of geological interface types in mining areas, by processing the boundary arc attribute information in digital geological maps, combining natural language processing and convolutional neural network training, the model identification accuracy reaches 96.52%, which effectively improves the efficiency of geological information extraction and the accuracy of the subsequent mineral prediction [15]. Daviran et al. integrated and optimized genetic algorithms and multiple machine learning for porphyry copper ore mineralization prediction and uncertainty quantification, successfully circled 12% of the low-risk target areas in the study area and encompassed 74% of the known deposits, which effectively improved the exploration efficiency and success rate [16]. El Alaoui El Fels et al. integrated remote sensing, geochemical data and logistic regression models to predict mineralization in the Bouazir ophiolite complex, Morocco, effectively identifying tectonically controlled cobalt-chromium-nickel anomalies and hydrothermal alteration, which significantly improved the exploration accuracy of locating copper-cobalt-nickel mineralization in oceanic crustal environments [17]. Zhibin et al. customized a comprehensive scheme integrating 3D

dynamic geological modeling and parallel visualization, combined with image processing techniques to extract core image features, and applied it to the case of a copper mine, effectively integrating multivariate data and significantly improving the accuracy and efficiency of quantitative assessment of mineral resources [18].

In this paper, three-dimensional structural model and raster model are constructed on the GOCAD platform from three levels of mining catchment area, mining area and deposit, which are converted to the available data format of GOCAD by Arcgis for modeling, and three-dimensional geological model is established by using the GOCAD software system. The three-dimensional mineralization prediction study was carried out with the X mining area as the study area, quantitatively analyzed the characteristic values of the mineralization element factors in the whole study area, applied the evidence weighting method to buffer and assign values to the rock body model of the block model, and evaluated the prediction validity and feasibility of the mineralization model by using the ROC curve analysis method and based on the AUC value.

2 3D Geological Modeling

2.1 3D Geological Modeling Process

(1) GOCAD software

The software platform used for modeling in this paper is GOCAD (Geological Object Computer AidedDesign), which is the main product developed and marketed by Earth Decision.GOCAD software has powerful 3D modeling, visualization, geological interpretation and analysis GOCAD software has powerful 3D modeling, visualization, geological interpretation and analysis functions. GOCAD software has powerful 3D modeling, visualization, geological interpretation and analysis functions. It can perform both surface modeling and solid modeling; it can design spatial geometric objects and express spatial attribute distribution.

GOCAD is a new generation of geological modeling software with workflow as the core, reaching the level of semi-intelligent modeling, with strong functions, easy to learn and use, friendly interface, and can run on almost all operating platforms.

(2) Kriging algorithm

Geostatistics mainly uses various unbiased optimal estimation methods, collectively known as kriging method (also known as kriging method), based on structural analysis (establishment of variance function) to estimate and solve practical problems, and according to the different research purposes and conditions, there are a variety of kriging methods have been produced, including simple kriging, ordinary kriging, pan kriging synergistic kriging, and instructed kriging, etc. . The valuation method used in this research is the ordinary kriging algorithm, the principle of which is briefly described below:

Let $Z^{(x)}$ be a regionalized variable, and assume that $Z^{(x)}$ obeys the second-order smoothness assumption, i.e., there is an expectation (Equation (1)), and a centered covariance function (Equation (2)) or a variance function (Equation (3)):

$$E[Z(x)] = m \tag{1}$$

$$E\{[Z(x+h) - Z(x)]^2\} = 2\gamma(h) \tag{2}$$

$$E\{Z(x+h)Z(x)\} - m^2 = C(h) \tag{3}$$

$$Z = \frac{1}{V} \int_{V(x)} Z(x)dx \tag{4}$$

Estimating the mean value (Eq. (4)) of the domain $V(x_0)$ centered at x_0, with a set of information values $\{Z_\alpha, \alpha = 1,2,\cdots,n\}$ around the domain to be estimated V, and their expectation $E\{Z_\alpha\} = m$ under second-order smoothing, the estimate Z^* of the actual value Z of the domain to be estimated V is a linear combination of these n valid data $Z_\alpha(\alpha = 1,2,\cdots,n)$ as Eq. (5):

$$Z^* = \sum \lambda_\alpha Z_\alpha \tag{5}$$

The n weighting factor $\lambda_\alpha(\alpha = 1,2,\cdots,n)$ in Eq. is derived in order to ensure that the estimator Z^* is unbiased and the estimated variance is minimized. The estimate Z^* computed from the weight coefficient λ_α is called the Kriging estimate of Z and the minimum estimation variance is called the Kriging variance and is denoted δ^2.

1) Unbiased condition. In order to avoid systematic errors, it is necessary to estimate unbiased, i.e., $E\{Z - Z^*\} = 0$. Under the second-order smooth condition (Eqs. (6), (7)), to make $E\{Z\} = E\{Z^*\}$, i.e., $m\sum \lambda_\alpha = m$ it is necessary to make $\sum \lambda_\alpha = 1$, i.e., the unbiased condition:

$$E\{Z\} = E\{Z^*\} = m \tag{6}$$

$$E\{Z^*\} = E\left\{\sum \lambda_\alpha Z_\alpha\right\} = \sum \lambda_\alpha E\{Z_\alpha\} = \sum \lambda_\alpha * m \tag{7}$$

$$\delta^2 = \bar{C}(V,V) - 2\sum_\alpha \lambda_\alpha \bar{C}(V, v_\alpha) + \sum_\alpha \sum_\beta \lambda_\alpha \lambda_\beta \bar{C}(v_\alpha, v_\beta) \tag{8}$$

2) Ordinary Kriging system of equations. Equation (8) is the formula for the estimated variance, under the unbiased condition, the estimated variance δ^2 to reach the very small weighted coefficients $\lambda_\alpha(\alpha = 1,2,\cdots,n)$ is a problem to find the conditional extreme value, in order to facilitate the solution, the very small $E\left\{\left[Z_V - Z^*\right]^2\right\}$ can be converted to the unconstrained Lagrange multiplier method to find the extreme value of the problem, that is, the constraints $\sum \lambda_\alpha = 1$ is also introduced into the objective function, so that:

$$F = \delta_E^2 - 2\mu\left(\sum_{\alpha=1}^{n} \lambda_\alpha - 1\right) \tag{9}$$

F is a $(n+1)$-element function with n power coefficients $\lambda_\alpha(\alpha = 1,2,\cdots,n)$ and μ, and -2μ is a Lagrange multiplier (the purpose is to make the equations obtained later simpler). The partial derivatives of F with respect to n $\lambda_\alpha(\alpha = 1,2,\cdots,n)$ and μ are found and

made 0 (equations (10), (11)). Finally the system of Kriging equations is obtained (Eq. (12)):

$$\begin{aligned} F &= \bar{C}(V,V) - 2\sum_{\alpha=1}^{n}\lambda_\alpha \bar{C}(V,v_\alpha) \\ &+ \sum_{\alpha=1}^{n}\sum_{\beta=1}^{n}\lambda_\alpha\lambda_\beta \bar{C}(v_\alpha,v_\beta) - 2\mu\left(\sum_{\alpha=1}^{n}\lambda_\alpha - 1\right) \end{aligned} \tag{10}$$

$$\begin{cases} \partial F / \partial \lambda_\alpha = 0 \\ \partial F / \partial \mu = 0 \end{cases} (\alpha = 1,2,\cdots,n) \tag{11}$$

$$\begin{cases} \sum_{\beta=1}^{n}\lambda_\beta \bar{C}(v_\alpha,v_\beta) - \mu = \bar{C}(v_\alpha,V) \\ \sum_{\alpha=1}^{n}\lambda_\alpha = 1 \end{cases} (\alpha = 1,2,\cdots,n) \tag{12}$$

3) Ordinary kriging variance. From equation (12), equation (13) can be obtained and substituted into the estimated variance equation (7), the minimum estimated variance, notation δ_K^2, equation (14):

$$\sum_{\beta=1}^{n}\lambda_\beta \bar{C}(v_\alpha,v_\beta) = \bar{C}(v_\alpha,V) + \mu \tag{13}$$

$$\begin{aligned} \delta_K^2 &= \bar{C}(V,V) - 2\sum_{\alpha=1}^{n}\lambda_\alpha \bar{C}(V,v_\alpha) + \sum_{\alpha=1}^{n}\sum_{\beta=1}^{n}\lambda_\alpha\lambda_\beta \bar{C}(v_\alpha,v_\beta) \\ &= \bar{C}(V,V) - \sum_{\alpha=1}^{n}\lambda_\alpha \bar{C}(V,v_\alpha) + \mu \end{aligned} \tag{14}$$

The Kriging algorithm is a method to estimate the grade of a block by considering the geometric features such as the size and shape of the information samples and their spatial distribution and positional relationship with the block to be evaluated, as well as the spatial structural and attribute features of the grade from the perspective of the correlation and variability of the variables, assigning a certain weighting coefficient to the value of each sample, and then finally carrying out a weighted average to estimate the grade of a block, so that it can carry out unbiased and optimal estimation of the value of a regionalized variable within a finite area. Unbiased and optimal estimation reflects the spatial structure and attributes of the variables, thus enabling statistical analysis and evaluation of the geological body.

(3) GOCAD modeling process

According to the establishment of the actual model, the three-dimensional modeling flow is summarized from the three levels of the mining catchment area, mining area and deposit as shown in Figure 1.

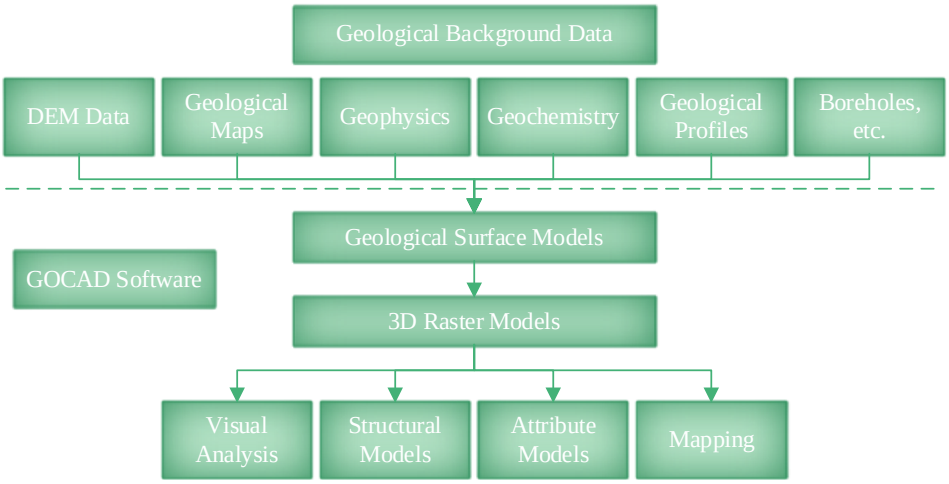

Figure 1: The lowchart of 3D geological modeling

2.2 Geological modeling

(1) 3D surface modeling

The data source for 3D surface modeling was the DEM elevation data of the study area. The used DEM data were imported into Arcgis to extract elevation points. Since the original elevation data range exceeds the study area range, in order to reduce the data volume and facilitate the subsequent data processing, the DEM data should be cropped before extracting the elevation points, and the size of the cropping is determined by the study area range vector data. The extracted elevation data were loaded into GOCAD software, and the surface model of the study area was established by using the structural modeling process, i.e., the Structural Modeling tool to create surfaces.

(2) Fault surface modeling

The faults are modeled based on the data obtained from the field work on the yield of the major faults in the study area and the fault surface trajectories. To accomplish this process in GOCAD, firstly, we can convert the fault surface properties collected from the field work into tangent vector (X,Y,Z). In GOCAD software system, X represents the value on the U-axis, with due east as the positive direction; Y represents the value on the V-axis, with due north as the positive direction; Z represents the value on the W-axis, with up as the positive direction. The following are the formulas for X, Y and Z:

$$X = \cos(\alpha)\cdot\sin(\beta) \tag{15}$$

$$Y = \cos(\alpha)\cdot\cos(\beta) \tag{16}$$

$$Z = -\sin(\alpha) \tag{17}$$

where the meaning of α indicates the dip of the fault trend, and the meaning of β indicates the inclination of the fault trend.

and ($0°\leq \alpha \leq 90°$, $0°\leq \beta \leq 360°$).

(3) Three-dimensional geologic body modeling

The lithological interface of the target geologic body extracted from the relevant geologic data in the study area was converted into point data and imported into GOCAD in the form of

Horizon Interpretations.

Create a Structure&Stratigraphy workflow in GOCAD and set the name of the workflow. Select the created lithological interface scatter file to start modeling, first create a stratigraphic column, second define the top and bottom surfaces of the geologic model of the study area to be created, and then create all the interfaces from the scatter. Next, the number of vertical and planar grids is set, in this work the number of grids is set to 100 x 100 x 10 grids, and finally the 3D geologic model grid is created. In addition, in order to make the color of each cell of the generated solid model meet the relevant requirements, it is necessary to set the color of the model for different geological cells, so that the 3D solid model is completed.

The horizontal and vertical variation functions of the grade data are shown in Fig. 2, where the nuggets in the vertical direction have small values, large variations, and better vertical continuity, while in the horizontal plane the nuggets have large values, short variations, and poor continuity.

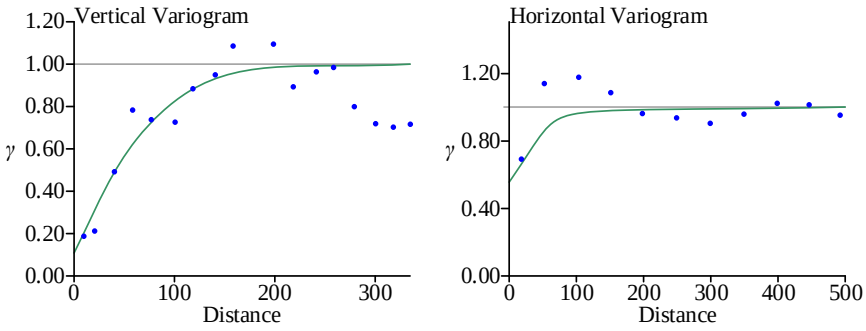

Figure 2: Level of Taste Data and Vertical Difference Function

2.3 Geological attribute modeling based on kriging methods

The purpose of this paper is to extract favorable two-dimensional geological information, establish three-dimensional solid model, integrate the spatial attribute relationship between the grade data of drill holes and rock samples, and use the DSI interpolation simulation and ordinary kriging algorithm of Gocad platform to derive the prediction model of the grade trend in the area, so as to provide the basis and method for the prediction and evaluation of the search for the blind ore bodies in the area.

The most direct way to verify the reliability of the grade model is whether the high value zone of the simulation results can be fitted with the spatial location of the gold ore body. If the fit is good, we should also pay attention to the correlation between the grade changes in the model and the geological factors, and the relationship with the tectonic zones, rock bodies (granodiorite and diorite porphyry), and the mineralized three-dimensional alteration zones.

3 Three-dimensional mineralization prediction based on three-dimensional geological models

3.1 Extraction of favorable information on mineralization

(1) Stratigraphic information extraction

According to the three-dimensional geological block model of the X mining area, the correlation analysis of different strata and known ore body blocks in the study area is carried out. The results of the research group's statistical analysis on the superposition of strata and ore blocks in the X mining area are shown in Fig. 3. The results of the superposition analysis on

different strata and known ore bodies show that the number of gold ore blocks in the strata is 4750, of which the number of gold ore blocks in Group 1 accounts for 47.9% of the number of gold ore blocks in the strata, therefore, the strata in the study area is a favorable formation for the formation of gold mines in this study area.

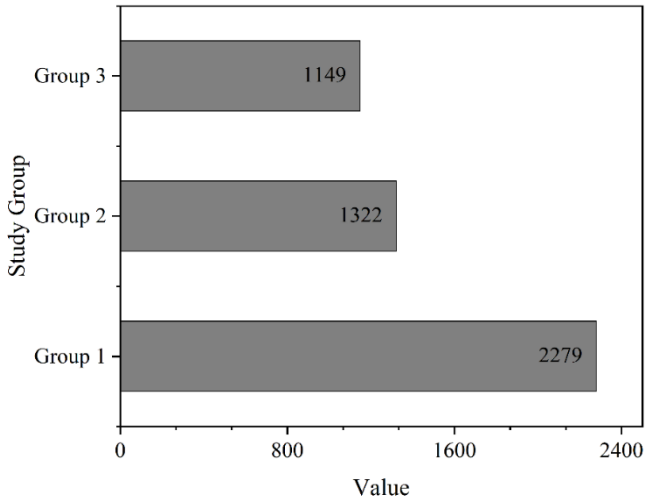

Figure 3: The Statistical Analysis of Overlapping between Strata and Ore Blocks

(2) Rock body information extraction

Calculate the relationship between the buffer zone range of the rock body and the known gold ore body units at different scales, so as to analyze the buffer zone range of the best rock body conducive to mineralization in the study area, and the results are shown in Figures 4 to 6. In the figure, the ratio refers to the ratio of the number of blocks of gold ore bodies contained in the corresponding rock body and the number of blocks of the unit within its buffer zone under the range to the overall number of blocks of gold ore bodies; and the ore-containing ratio refers to the ratio of the number of ore-containing blocks to the number of blocks. From the characteristics analysis of the number of ore-bearing nuggets under the buffer range of different rock bodies, it can be seen that: the buffer zone of 20m of fractured rock is the best favorable range of fractured rock, the buffer zone of 80m of quartz schist is the best favorable range of quartz schist, and the buffer zone of 145m of dioritic granite is the best favorable range of dioritic granite.

(1) The best buffer zone of fractured rock

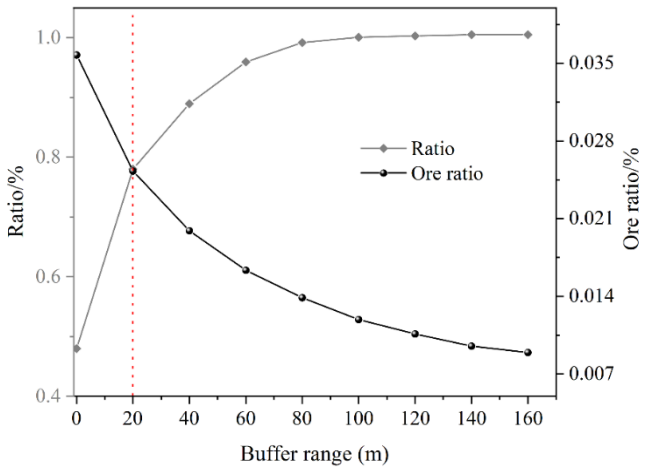

Figure 4: Statistical line graph of superposition of fractured rock buffer and ore body

2) Quartz schist optimal buffer

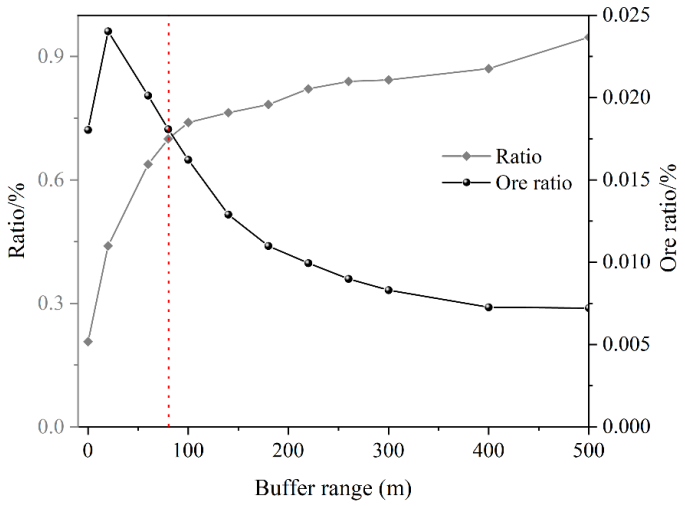

Figure 5: Statistical line graph of quartz schist and ore body superposition

3) Optimal buffer analysis for plagioclase granite

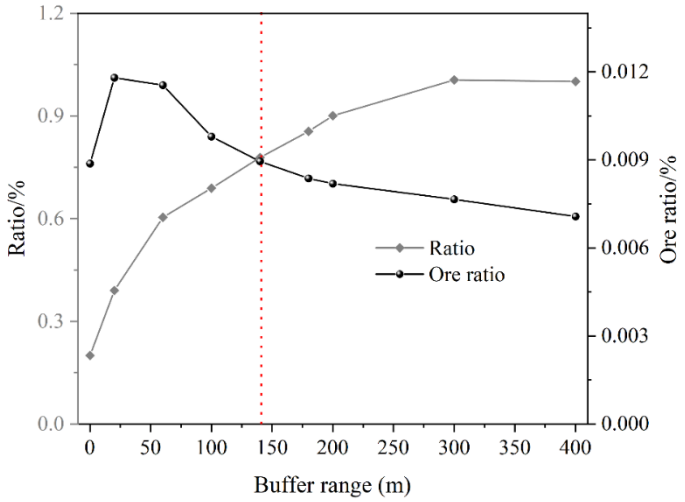

Figure 6: Line Graph of Overlapping Statistics between Diabase Buffer and Ore Body

(3) Tectonic information extraction

Fracture structure plays a crucial role in the metallogenesis of the X mining area, through the superposition analysis of these characteristic variables and the known ore bodies in the region, quantitative analysis describes the various characteristics of the structure to extract favorable information for metallogenesis, thus providing a data basis for the mineral prediction and evaluation work.

The tectonic activity in the region is strong, and the deep and large fractures in the region provide transportation channels for the movement of mineral materials, and a large number of brittle fractures formed in a certain space around the large-scale fractures constitute a well-enclosed space for mineralization. Therefore, the fracture structure and a certain range of three-dimensional space around the fracture structure play an important role in the formation of the gold ore body in the district. Different sizes of buffer zones are analyzed for the fractures, and the statistical results of the superposition of the fracture buffer zones and the ore body at different scales are statistically analyzed, as shown in Figure 7. The 20m buffer zone of the

selected fracture is the best mineralization buffer zone range analyzed by the statistical results. Therefore, the fracture and the 20m buffer zone of the fracture are selected as favorable mineralization factors.

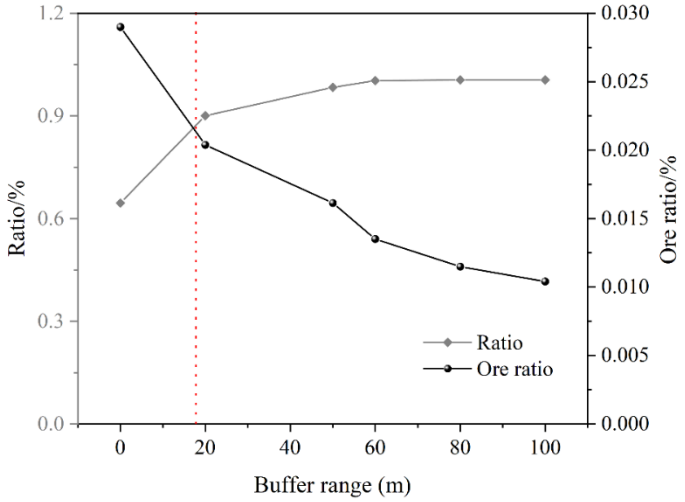

Figure 7: Analysis and Statistics of Broken Buffer and Ore Deposit Overlapping Line Graph

3.2 Three-dimensional right to evidence approach

(1) Principle of the three-dimensional weight-of-evidence method

First of all, the information in the block unit is comprehensively organized and quantified, and the formula of the right of evidence method is used to sum up the weights of the favorable mineralization factors in each block unit in the block model and calculate the a posteriori probability of the block unit, whose value represents the magnitude of the possibility of containing minerals in the area. When the critical value of the a posteriori probability of the prediction area is determined, the place where the a posteriori probability of mineralization is greater than the critical value in the block model is classified as a high-value area, i.e., it is regarded as the target area for finding minerals.

The a priori probability is calculated by dividing the volume in the region uniformly into T block cell, and the number of block cells containing ore in T block cells in the block model is D, P is the probability that the block cell contains an ore body when a cell in the block model is arbitrarily selected. That is, the formula for the a priori probability is:

$$P_{\text{A priori}} = P(D) = \frac{D}{T} \tag{18}$$

A priori odds O for:

$$O_{\text{A priori}} = O(D) = \frac{P(D)}{1-P(D)} = \frac{D}{T-D} \tag{19}$$

$O_{\text{A priori}}$ (a priori favorability) to calculate the ratio of the a priori probability of ore-bearing block units to those that are not ore-bearing for each mineralizing geologic factor attribute.

$$W^+ = \ln \frac{P(B/D)}{P(B/\bar{D})} = \ln \frac{N(B \cap D)/N(D)}{(N(B) - N(B \cap D))/(N(T) - N(D))} \tag{20}$$

$$W^- = \ln \frac{P(\bar{B}/D)}{P(\bar{B}/\bar{D})} = \ln \frac{(N(D) - N(B \cap D))/N(D)}{(N(T) - N(B) - N(D) + N(B \cap D))/(N(T) - N(D))} \tag{21}$$

In the formula, W^+ means that the weight value of each attribute of mineralizing geological factors exists in the prediction area, and W^- means that the weight value of each attribute of mineralizing geological factors does not exist in the prediction area. If the weight value is 0, it means that the data are missing in the prediction area. B and $\bar{B}$ represent the number of occurrences or absences of each mineralizing geological attribute in the layer.

$$C = W^+ - W^- \tag{22}$$

The value of C represents the degree of favorability of mineralization between the attributes of the mineralizing geological factors and the attributes of the ore body.

When the value of C > 0, it means that the property of the mineralizing geological factor is favorable for mineralization, and the location of the target area can be predicted quantitatively.

When the value of C =0, it means that the mineralizing geological attribute has no significance in guiding the mineralization.

When the value of C is <0, it means that the attribute of the mineralization geological factor is not conducive to mineralization and should be discarded.

Based on C to select the reasonable mineralization geological factor layer, and carry out the conditional independence test. Based on the conditional independence test of X^2, if the value of C is less than 0.05, it means that there is no conditional independence between the layers of mineralizing geological factors.

$$\ln\left(O\left(D\middle|B_1^k \cap B_2^k \cap B_3^k \cdots B_n^k\right)\right) = \sum_{j=1}^{n} W_j^k + \ln\left(O(D)\right) \tag{23}$$

The a posteriori chances are:

$$O_{\text{A posteriori}} = \exp\left\{\ln\left(O_{\text{A priori}}\right) + \sum_{j=1}^{n} W_j^k\right\} \tag{24}$$

$$P(D/B) = \frac{\exp\left(L(D/B)\right)}{1 + \exp\left(L(D/\bar{B})\right)} \tag{25}$$

$$L(D/B) = L(D) + W^+ \tag{26}$$

$$L\left(D/\bar{B}\right)=L\left(D\right)+W^{-} \tag{27}$$

The a posteriori probability is:

$$P_{\text{A posteriori}}=\frac{O_{\text{A posteriori}}}{\left(1+O_{\text{A posteriori}}\right)} \tag{28}$$

Using the above formula to bring into the block model, through the graphic interpolation constraint function in 3Dmine software, assign values to each favorable mineralization element attribute, calculate the positive and negative weight values and a posteriori probability. Superimpose the positive weight value of each favorable mineralization element attribute to derive the a posteriori probability value of the mine, the a posteriori probability value should be between 0 and 1, and the a posteriori probability value is positively correlated with the probability of mineralization.

(2) Establishment of evidence weight model

In this paper, combined with 3Dmine software, the calculation of the evidence weight model is summarized in accordance with its principle, which mainly includes three elements: ① In the block model, search for blocks containing ore bodies in the region, assign the value of block cells containing ore bodies to 1, and assign the value of block cells not containing ore bodies to 0, and statistically report the number of block cells containing ore bodies in the whole. ② The spatial characteristics of the attributes of each mineralizing geological factor are constrained by zoning, and the zoning is based on the distance from the ore body at intervals of 50m, and the buffer zone is established, i.e., the spatial influence range of the geological factor. ③ Calculate the W^{+}, W^{-} and C values of each unit block according to the above formula; ④ Superimpose the W values of the 50m sub-zones of each mineralizing geological factor attribute, calculate the value of a posteriori probability in each block unit on the basis of a posteriori probability, and arrive at the ratio of each mineralizing element to the block, and finally circle the predicted favorable area for metallogenesis based on the high-value area of the a posteriori probability.

(3) Three-dimensional weight of evidence calculation

The attribute names of the metallogenic element factor thematic layers in the model are North-North-West (NNW) faults, South-North (SN) faults, and North-East-South-West (NE-SW). The positive weight value (W^{+}), negative weight value (W^{-}), and comprehensive weight value (C) of the metallogenic element factors within the weight-of-evidence model are calculated according to the above formula, and the weight values of each metallogenic element are shown in Tables 1 to 3.

From the table, it can be seen that the positive weighting values of the north-northwest (NNW) fault structure are all greater than 1 except for the distance of 50m from the tectonic zone, and the positive weighting values between 100m and 450m are closer to about 2. Based on the proportion of the ore block and the W+ value, a buffer zone is delineated between 100m and 450m. This interval has an obvious positive influence on the formation and enrichment of the ore body. The positive weight value of the north-south (SN) fault structure is larger, and the positive weight value between 50m and 200m from the tectonic zone is more than 2, and it reaches more than 3 when 0m to 50m from the tectonic zone, which indicates that this subzone has a strong guiding significance on ore search and is closely related to mineralization. The North-East-South-West (NE-SW) fault has a greater positive weight value as the distance from the sub-belt increases. The data changes are more obvious between 700m and 950m, and the positive weight value and the integrated weight value in the interval are above 1, indicating that

the fault plays a certain role in mineralization, so 700m to 950m is designated as its tectonic buffer zone.

Table 1: NNW Fault Buffer Weight Table

NNW	Total blocks	Number of ore-bearing blocks	W^+	W^-	C	Sort
0m~50m	472509	505	0.3437	-0.0095	0.3274	60
50m~100m	517707	1237	1.3167	-0.0429	1.3419	48
100m~150m	526123	2080	1.8405	-0.0816	1.9044	38
150m~200m	542187	2784	2.11	-0.1149	2.2072	33
200m~250m	556319	3181	2.2207	-0.134	2.337	22
250m~300m	573038	3730	2.3536	-0.1612	2.4971	18
300m~350m	584009	3558	2.2863	-0.1522	2.4208	20
350m~400m	591356	2994	2.0972	-0.1238	2.2034	34
400m~450m	592072	2290	1.821	-0.0898	1.893	40
450m~500m	599949	1166	1.1069	-0.0375	1.1266	54

Table 2: Northbound (SN) fault buffer weight

SN	Total blocks	Number of ore-bearing blocks	W^+	W^-	C	Sort
0m~50m	484006	6788	3.1356	-0.3333	3.4712	4
50m~100m	559582	6467	2.9391	-0.312	3.2535	8
100m~150m	551343	5447	2.779	-0.2535	3.0348	10
150m~200m	559618	3213	2.225	-0.1355	2.3628	21
200m~250m	567332	1162	1.1593	-0.0382	1.1997	51

Table 3: Weight value of the moderate fault zone in the northeast-southwest (NE-SW) direction

NE-SW	Total blocks	Number of ore-bearing blocks	W^+	W^-	C	Sort
600m~650m	306998	267	0.1238	-0.0056	0.1287	62
650m~700m	307108	461	0.7738	-0.0141	0.7872	58
700m~750m	307229	604	1.0757	-0.0203	1.0953	55
750m~800m	307254	646	1.1494	-0.0222	1.1709	53
800m~850m	307253	793	1.372	-0.0287	1.4234	47
850m~900m	307539	1116	1.7352	-0.0431	1.7776	45
900m~950m	307459	1144	1.7616	-0.045	1.8059	44

Calculate the ore block ratio of each mineralization element (i.e., the ratio of the number of ore-bearing unit blocks to the total number of ore-bearing unit blocks in the a posteriori probability intervals within the attributes of each mineralization geological element) as shown in Table 4, in which it can be seen that most of the ore-bearing blocks are distributed in the interval of the a posteriori probability value of 0.95 to 1.00, and the total number of ore-bearing unit blocks in the study area is 24,136, and the number of ore-bearing units in the interval of 0.95 to 1 is 20222 and the ore block ratio is 83.7836%. So the a posteriori probability value between 0.95 and 1 is taken as a high value zone and is used to classify it as a favorable zone for finding ore.

Table 4: mineral block ratio of posterior probability in mineral block

Posterior probability interval	Ore block	Block count	Block ratio (%)	Posterior probability interval	Ore block	Block count	Block ratio (%)
0~0.05	87	3.41132E7	0.3605	0.5~0.55	147	60668	0.6091
0.05~0.1	134	814054	0.5552	0.55~0.6	133	214011	0.5510
0.1~0.15	49	322331	0.2030	0.6~0.65	87	135004	0.3605
0.15~0.2	93	43063	0.3853	0.65~0.7	110	182257	0.4558
0.2~0.25	64	53404	0.2652	0.7~0.75	98	15695	0.4060
0.25~35	170	101885	0.7043	0.75~0.8	225	16242	0.9322
0.3~0.35	229	84003	0.9488	0.8~0.85	687	45575	2.8464
0.35~0.4	257	93383	1.0648	0.85~0.9	736	125214	3.0494
0.4~0.45	143	220103	0.5925	0.9~0.95	269	327451	1.1145
0.45~0.5	196	68206	0.8121	0.95~1	20222	386076	83.7836

(4) Performance evaluation indicators of mineralization prediction models

The area under the ROC curve, namely the AUC value, is a quantitative evaluation indicator that is independent of the threshold. It is a comprehensive evaluation indicator for measuring the prediction effect of different methods and models. The larger the AUC value, the better the prediction effect of the model. When the AUC value of model accuracy is greater than 0.9, it can be determined that the model prediction effect is excellent. When the value is between 0.8 and 0.9, the model prediction effect is good. When the value is between 0.7 and 0.8, the model prediction effect is average. When the value is between 0.6 and 0.7, the model prediction effect is poor. When the value is between 0.5 and 0.6, it indicates that the classifier is similar to random guessing and has no predictive value.

$$AUC = \frac{1}{ab}\sum_{i=1}^{a}\sum_{j=1}^{b}\varphi\left(x_i, y_j\right) \tag{29}$$

$$\varphi\left(x_i, y_j\right) = \begin{cases} 1 & x_i > y_j \\ 0.5 & x_i = y_j \\ 0 & x_i < y_j \end{cases} \tag{30}$$

3.3 Determination of Target Areas for Ore Searching

(1) Model performance analysis

Figure 8 shows the prediction performance of the ROC curve and the mineralization rate curve of the weight-of-evidence method. In the figure, the AUC value of the weight-of-evidence method is 0.94, and its high a posteriori probability part has higher sensitivity to the mineralization category and higher prediction accuracy for the mineralization category.

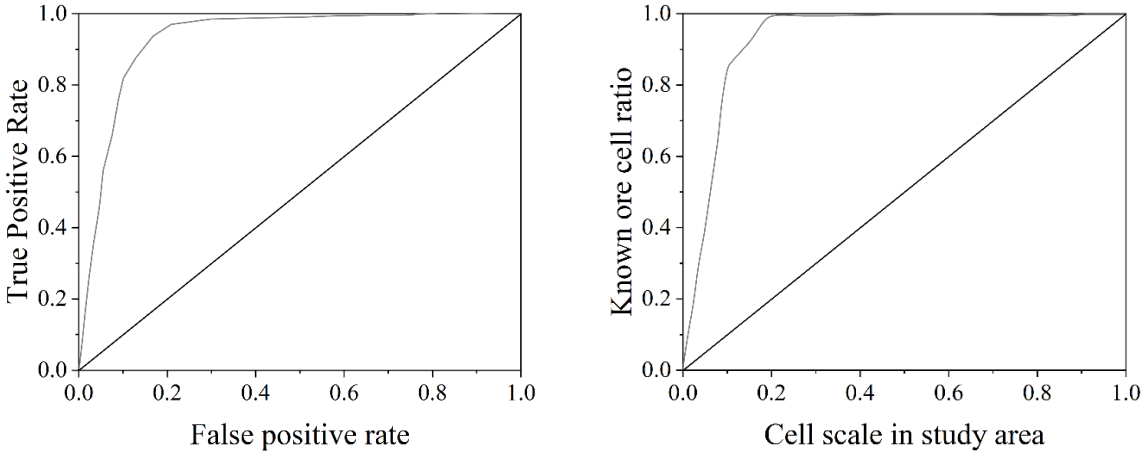

(a) ROC curve (b) Ore-forming rate curve

Figure 8: Performance Prediction Results

(2) Weight-of-evidence method target area circling

The a posteriori probability is a key indicator for describing the mineralization potential of an area, representing the possibility of mineralization for each body element. The best probability threshold was determined to be 0.50 by statistical analysis of the a posteriori probability to distinguish between the X mining area region and the background. Fig. 9 shows the X mining area region and the circled target areas obtained from the prediction of the weight-of-evidence method, and a total of four mineralized target areas were circled: target area A, target area B, target area C and target area D. Combined with the geological background of the metallogenic zone and the scale of mineralization, target area A is not only relatively large, but also contains most of the body elements with high a posteriori probability, which can be classified as class I target area. The second relatively large target area is target area B, which contains voxels with lower a posteriori probability compared with target area A, and can be classified as class II target area. Finally, target area C and target area D, with smaller scale and low a posteriori probability of containing body elements, are class III target areas. Their a posteriori probability of mineralization can be classified into four levels: high, higher, lower, and low, in which the high probability area is mainly distributed in the vicinity of known ore-bearing cells in target area A, the higher probability area is distributed in target area A, and the lower probability and low probability are mainly distributed in target areas B, C, and D.

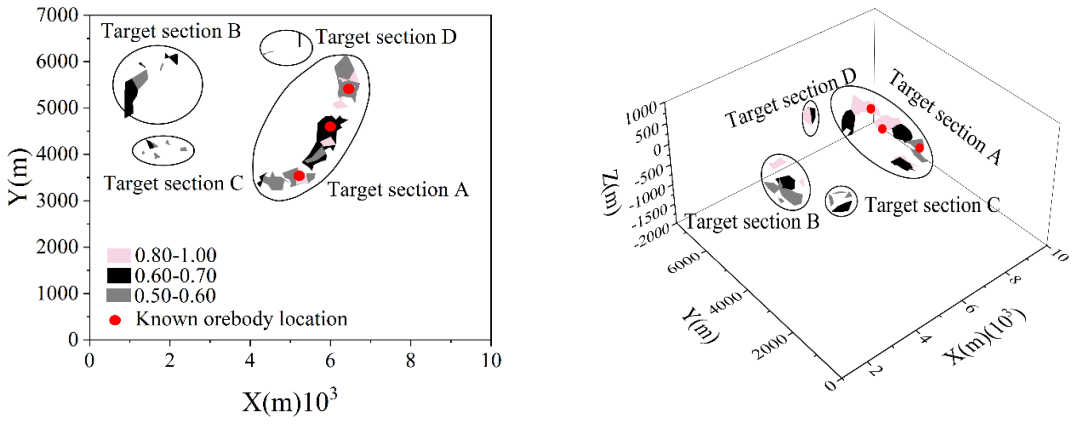

(a) Vertical view (b) Lateral view

Figure 9: High prospect area of metallogenic potential obtained by evidence weight method

The surface gold anomalies of the X mining area and the location of the target area are schematically shown in Figure 10, and it can be seen that the location has a good mineralization background.

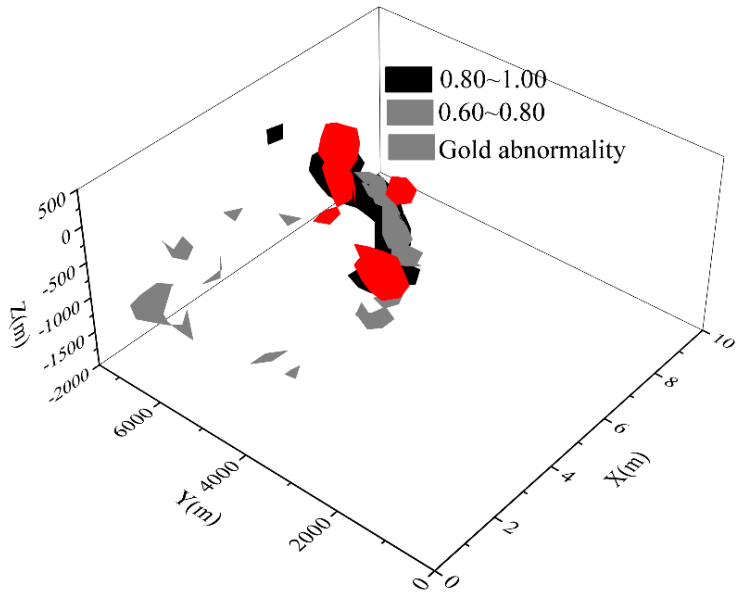

Figure 10: Schematic diagram of surface gold anomaly and target area location

(3) Evaluation of mineralization prediction model

The process of mineralization prediction and evaluation is affected by many factors, such as the completeness of the regional data, the reliability of the working method, the accuracy of the actual engineering exploration, etc. Therefore, the results of the mineralization prediction are evaluated with "fixed probability". The expert scoring and weighting method is used to evaluate the entire three-dimensional mineralization prediction process in the study area, and the expert scoring and weighting method is a quantitative assessment of the reliability of the original data base, the degree of work in the study area, and the mineral search model.

In summary, according to the expert scoring weighting method and the assignment of each evaluation factor as shown in Table 5, therefore, according to the calculation formula of the expert scoring weighting method:

$$P = W_i \times V_i \tag{31}$$

where P is the synthesized value of the probability of finding ore, W_i is the weight value of the evaluation element factor i, and V_i is the scoring value of the evaluation element factor i. Evaluation of the accuracy of three-dimensional mineralization prediction in the study area can be calculated as 78.2% probability of finding ore. Although the accuracy of the data in the study area is relatively high, the type of data used in the study is relatively small, so there is a certain risk in the prediction and evaluation work, but on the whole, the prediction results have a high degree of confidence, and it is possible to carry out the practice of mineral prospecting and exploration in this area.

Table 5: Evaluation factor assignment and weight table

Evaluation factor	V_i	W_i
Data base	0.84	0.27
Workload	0.91	0.22
Predictive unit	0.62	0.11
Mineral exploration model	0.59	0.31
Positioning accuracy	0.81	0.16
Probabilistic prospecting	0.782	

4 Conclusion

The study constructed a three-dimensional geological model on the GOCAD platform, and used the kriging interpolation method to derive the grade trend prediction model in the district, and achieved the following results in the course of the study on the prediction of mineralization in the X mining district:

(1) Based on the three-dimensional geological entity model to divide the whole X mining area, quantitative extraction and analysis of the eigenvalues of the mineralization factors in the study area, and summarized the quantitative prediction model of gold mineralization in the area.

(2) Based on the established block model, the deep ore bodies in the Dulong mining area were predicted by assigning values to the block model using the weight-of-evidence method and the informativeness method. According to the statistical results of the weight-of-evidence method, the total number of ore-bearing unit blocks in the study area is 24,136, and the ratio of the blocks in the interval of a posteriori probability value of 0.95 to 1 is 83.7835%.

(3) The predictive performance of the weight-of-evidence method is evaluated using the ROC curve. The results show that the AUC value of the three-dimensional weight-of-evidence model is equal to 0.94, indicating that the model is indicative of deep mineral search in the study mine area.

(4) The probability evaluation of the prediction work in the study area was carried out systematically, and the evaluation value of the probability accuracy of this prediction work for finding ore was 78.2%.

References

[1] Okada, K. (2022). Breakthrough technologies for mineral exploration. Mineral Economics, 35(3-4), 429.

[2] Omotehinse, A. O., & Ako, B. D. (2019). The environmental implications of the exploration and exploitation of solid minerals in Nigeria with a special focus on Tin in Jos and Coal in Enugu. Journal of sustainable mining, 18(1), 18-24.

[3] Guo, X., Fan, N., Liu, Y., Liu, X., Wang, Z., Xie, X., & Jia, Y. (2023). Deep seabed mining: Frontiers in engineering geology and environment. International Journal of Coal Science & Technology, 10(1), 23.

[4] Gonzalez-Alvarez, I., Gonçalves, M. A., & Carranza, E. J. M. (2020). Introduction to the special issue challenges for mineral exploration in the 21st century: Targeting mineral deposits under cover. Ore Geology Reviews, 126, 103785.

[5] Levin, L. A., Amon, D. J., & Lily, H. (2020). Challenges to the sustainability of deep-seabed mining. Nature Sustainability, 3(10), 784-794.

[6] Okada, K. (2021). A historical overview of the past three decades of mineral exploration technology. Natural Resources Research, 30(4), 2839-2860.

[7] Sillitoe, R. H. (2024). 7. SUCCESS AND CHALLENGES IN MINERAL EXPLORATION. Geochemical Perspectives, 13(1), 141-167.

[8] Cao, X., Liu, Z., Hu, C., Song, X., Quaye, J. A., & Lu, N. (2024). Three-dimensional geological modelling in earth science research: an in-depth review and perspective analysis. Minerals, 14(7), 686.

[9] Zhang, Z., Zhang, J., Wang, G., Carranza, E. J. M., Pang, Z., & Wang, H. (2020). From 2D to 3D modeling of mineral prospectivity using multi-source geoscience datasets, Wulong Gold District, China. Natural Resources Research, 29(1), 345-364.

[10] Chen, J., Jiang, L., Peng, C., Liu, Z., Deng, H., Xiao, K., & Mao, X. (2023). Quantitative resource assessment of hydrothermal gold deposits based on 3D geological modeling and improved volume method: Application in the Jiaodong gold Province, Eastern China. Ore Geology Reviews, 153, 105282.

[11] Krassakis, P., Pyrgaki, K., Gemeni, V., Roumpos, C., Louloudis, G., & Koukouzas, N. (2022). GIS-based subsurface analysis and 3D geological modeling as a tool for combined conventional mining and in-situ coal conversion: the case of Kardia Lignite mine, western Greece. Mining, 2(2), 297-314.

[12] Lyu, P., He, L., He, Z., Liu, Y., Deng, H., Qu, R., ... & Wei, Y. (2021). Research on remote sensing prospecting technology based on multi-source data fusion in deep-cutting areas. Ore Geology Reviews, 138, 104359.

[13] Liu, Q., Chen, L., & Liu, J. (2025). Multi-source data fusion and 3D model construction for mines considering ISS+ ICP registration algorithm. Engineering Research Express, 7(4), 0452a3.

[14] Zhou, F., & Liu, L. (2025). Machine Learning Prediction of Deep Potential Ores and its Explanation Based on Integration of 3D Geological Model and Numerical Dynamics Simulation: An Example from Dongguashan Orefield, Tongling Copper District, China. Natural Resources Research, 34(1), 121-147.

[15] Zong, Y., Xue, L., Wang, J., Wang, P., & Ran, X. (2025). Research on Deep Learning-Based Identification Methods for Geological Interface Types and Their Application in Mineral Exploration Prediction—A Case Study of the Gouli Region in Qinghai, China. Minerals, 15(12), 1281.

[16] Daviran, M., Ghezelbash, R., Hajihosseinlou, M., & Maghsoudi, A. (2025). Uncertainty quantification in genetic algorithm-optimized artificial intelligence-based mineral prospectivity models: automated hyperparameter tuning for support vector machines and random forest. Modeling Earth Systems and Environment, 11(1), 10.

[17] El Alaoui El Fels, A., Hajaj, S., El Ghorfi, M., & Soulaimani, A. (2025). Enhanced

mineral targeting by using artificial intelligence-based modelling: remotely sensed and geochemical data for harnessing Co-Cr-Ni, and cupriferous mineral prospectivity mapping in Bou Azzer inlier (Central Anti-Atlas, Morocco). Earth Science Informatics, 18(4), 1-20.

[18] Zhibin, R., Zhian, W., Jianfeng, Q., & Qirui, N. (2025, May). Application of Visualization and Image Processing Algorithm of Geological Exploration Data in Mineral Resources Evaluation. In 2025 2nd International Conference on Telecommunications and Power Electronics (TELEPE) (pp. 517-521). IEEE.